


PAPER • OPEN ACCESS

A high quality surface finish grinding process to produce total reflection mirror for x-ray fluorescence analysis

To cite this article: Hitoshi Ohmori *et al* 2020 *Int. J. Extrem. Manuf.* **2** 015101

View the [article online](#) for updates and enhancements.

A high quality surface finish grinding process to produce total reflection mirror for x-ray fluorescence analysis

Hitoshi Ohmori¹, Shinjiro Umezu^{1,2}, Yunji Kim¹, Yoshihiro Uehara¹, Hiroshi Kasuga¹ , Teruko Kato¹, Nobuhide Itoh^{1,3}, Syuhei Kurokawa⁴, Takayuki Kusumi⁵, Yugo Sugawara⁶ and Shinsuke Kunimura⁶

¹ Materials Fabrication Laboratory, RIKEN, Saitama 351-0198, Japan

² Department of Modern Mechanical Engineering, Waseda University, Tokyo 169-8555, Japan

³ Department of Mechanical Systems Engineering, Ibaraki University, Ibaraki 316-8511, Japan

⁴ Department of Mechanical Engineering, Kyushu University, Fukuoka 819-0395, Japan

⁵ New technology developments, Akita Industrial Technology Centre, Akita 010-1623, Japan

⁶ Department of Industrial Chemistry, Tokyo University of Science, Tokyo 162-8601, Japan

E-mail: ohmori@mfl.ne.jp

Received 23 August 2019, revised 9 January 2020

Accepted for publication 26 February 2020

Published 16 March 2020



Abstract

Total reflection x-ray fluorescence analysis is applied to trace element detection in liquid for effective environmental monitoring. This analytical approach requires x-ray total reflection mirrors. In order to achieve high sensitivity element detection, the mirrors require high surface quality for high x-ray reflectivity. Surface finishing for x-ray mirrors is typically conducted through a series of abrasive processes, such as grinding and polishing, and is thus time consuming. The purpose of this study is to streamline and enhance the surface finishing process based on unique high quality grinding techniques for the production of x-ray total reflection mirrors.

Keywords: grinding, finishing, x-ray mirror

1. Introduction

X-ray mirrors, reflective optical elements that can reflect and focus x-ray (beams) of short wavelengths, are applied to various types of analyzers, including synchrotron radiation facilities [1], portable x-ray elemental analyzers [2], and astronomical x-ray telescopes [3]. In order to effectively characterize the optical and physical properties of x-rays, high surface precision at sub-nanometer (nm) levels of mean roughness [4] in various types of mirror geometry is necessary. Additionally, hard and brittle materials such as monocrystalline Si, quartz, SiC, and low heat-expansion glass, are

typically used [5], which makes achieving the required surface precision challenging. Furthermore, finishing processes for x-ray mirrors [6, 7] should be considered enough to be efficient.

The combination of ultraprecision grinding with electrolytic dressing [8] and specific polishing, such as elastic emission machining (EEM) [9], has been attempted in creating a mirror. The mirror will be shaped efficiently by grinding and both ground waviness and roughness will be diminished by EEM. Through this process combination, elliptical x-ray mirrors for x-ray free electron laser (X-FEL) facilities that can focus a trajectory of x-ray beam into an ultrafine spot of approximately 75 nm have been successfully produced [10].

Furthermore, portable x-ray elemental analyzers [2, 11] have been constructed based on total reflection x-ray fluorescent (TXRF) analysis [12], which are used in multiple fields



Original content from this work may be used under the terms of the [Creative Commons Attribution 3.0 licence](https://creativecommons.org/licenses/by/3.0/). Any further distribution of this work must maintain attribution to the author(s) and the title of the work, journal citation and DOI.

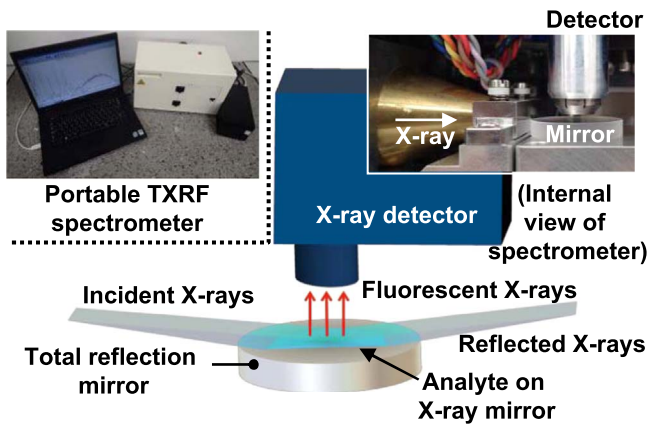


Figure 1. Portable TXRF spectrometer and its configuration.

that call for ultra trace analysis and high quality mirrors. Such mirrors are of plane (flat) geometry and small in size, requiring increased productivity due to their cost restrictions. The mirrors are also required to be accurately flat and smooth, at less than few nm in mean roughness. Materials for the mirrors can be chosen among Si, glassy carbon, and quartz glass. The strict requirements detailed above suggest that an innovative new finishing process that will maintain process number at a reasonable state, as well as attain the prescribed surface roughness and quality within a limited timeframe, is imperative. Therefore, in this study, we have developed a new grinding technique that will provide an efficient finishing process, which will allow for the practical manufacturing of total reflection mirrors dedicated to portable TXRF spectrometers.

2. Portable total reflection x-ray fluorescence spectrometer

Figure 1 displays the developed portable TXRF spectrometer [11] and its configuration. When the incident x-rays are totally reflected on the x-ray mirror, atoms in the analyte are excited by both the incident and reflected x-rays, resulting in the emissions of fluorescent x-rays. Then, the emitted fluorescent x-rays will be analyzed via the x-ray detector, producing a spectrum of the analyte compositions. Figure 1 also includes an internal view of the portable TXRF spectrometer. An x-ray tube with a tantalum anode was employed as the x-ray source, and quartz glass was used for the mirror.

3. Grinding characteristics of quartz mirror

3.1. Grinding method, experimental set-up and conditions

A precision grinding with electrolytic dressing process [8] was applied to finish mirrors; figure 2 illustrates the experimental grinding set-up, which was developed in our previous research. A rotary surface grinder, with air hydrostatic bearings for the

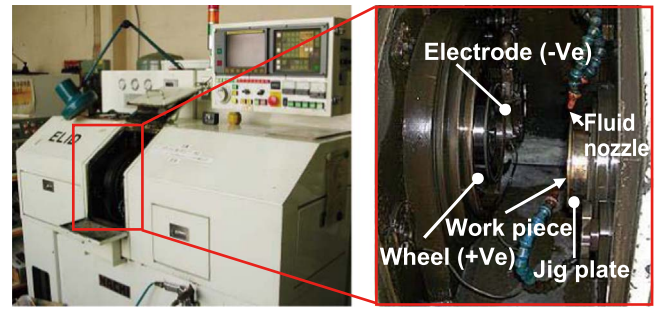


Figure 2. View of experiment set-up for grinding.

wheel and work piece spindles, was employed for the experiment. Detailed specifications of the set-up and grinding conditions are shown in table 1. The surface roughness (profile) was evaluated by the optical surface measuring instrument at five points on each work piece (mirror), and was then averaged to be compared to different wheels and finishing methods. After grinding, CMP (chemical mechanical polishing) was added to reduce grinding marks.

3.2. Grinding wheels

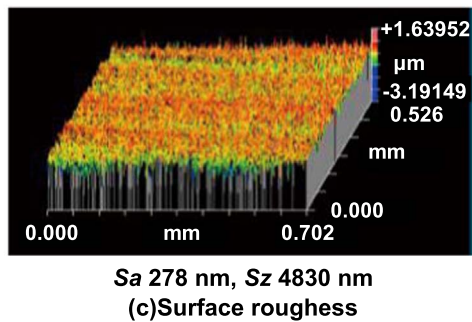
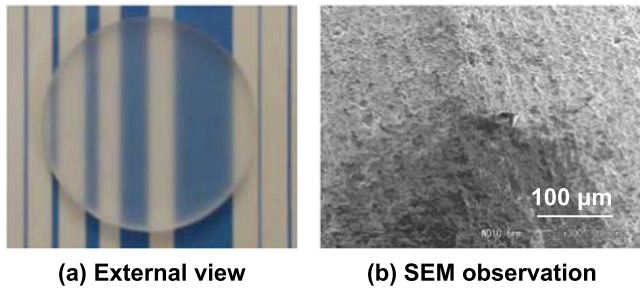
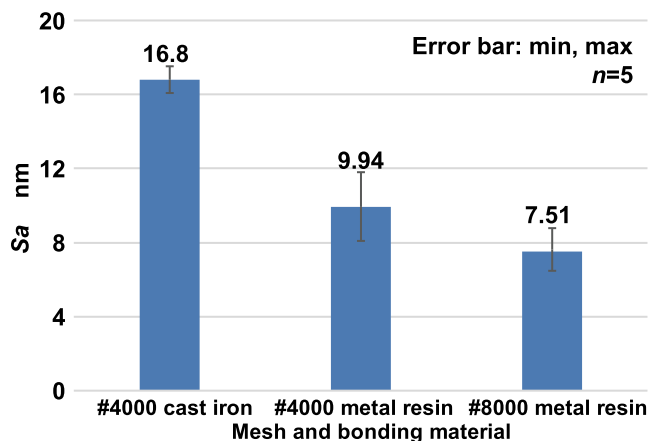
The application of several types of diamond grinding wheels were attempted for finishing the total reflection mirrors. Metal (cast iron) and metal resin compound bond grinding wheels were used for the experiments. Nano-diamond (ND) particles of ~ 4.9 nm in diameter were mixed with #20000 diamond abrasives at 2% volume in order to reduce the ground surface roughness of mirrors. A #325 wheel was utilized for preparation of mirror blanks.

3.3. Ground surface roughness due to grinding wheel

Figure 3 exhibits the surface quality of blanks produced by the #325 wheel, which appears to have been generated in brittle fracture mode (surface roughness: 278 nm). Its external view suggests that its optical property is poor. Then, the arithmetical mean height (S_a) and maximum height of scale limited surface (S_z) data, which were produced with #4000 metal (cast iron) bond wheels and with #4000, #8000 metal resin bond wheels, were evaluated, as detailed in figure 4. Compared to metal (cast iron) bond wheels, metal resin bond wheels can more effectively reduce roughness. S_a and S_z were 9.94 nm and 346 nm, respectively, after applying a #4000 metal resin bond wheel; however, a #8000 metal resin bond wheel was able to achieve an S_a and S_z of 7.51 nm and 194 nm, respectively. The surface profile examples produced by the #4000 wheels with different bond materials are displayed in figure 5. The metal resin bond was once again able to produce a smoother surface roughness, as confirmed by figure 5(b). The surface profile produced by the #8000 metal resin wheel bond is shown in figure 6, which displays a high quality transparent surface.

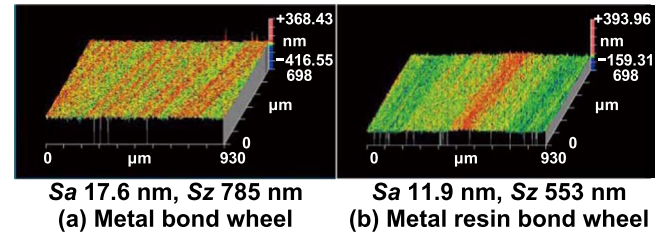
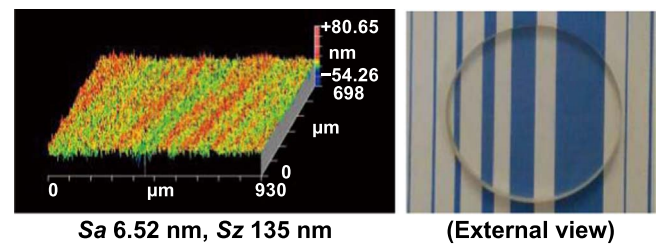
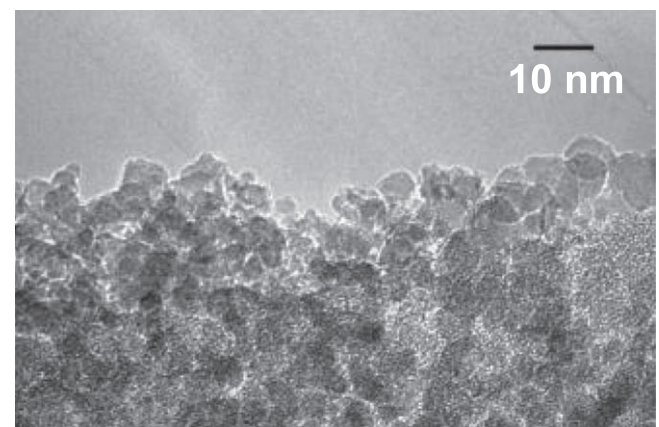
Table 1. Specifications of experimental set-up and grinding conditions.

| | | | |
|-----------------------|---|-----------------------|--|
| Grinding machine | Horizontal rotary in-feed grinder with air-hydrostatic bearings for grinding and work piece spindles | | |
| Grinding wheel | Cup type of $\varphi 143$ mm, width 3 mm; SD325, SD4000 metal (cast iron) bond, SD4000, SD8000 metal resin bond, and SD20000 metal resin bond with ND0%, 2% | | |
| Work piece | Quartz glass plate: $\varphi 30$ mm, t5 mm (initial surface was conventionally polished) | | |
| Grinding conditions | Wheel rotation | 900 m/min | |
| | Work piece rotation | 300 min ⁻¹ | |
| | Open voltage | 60 V | |
| | Peak current | 5 A | |
| | Pulse wave | Square | |
| Electrical conditions | dressing | Pulse timing | $\tau_{on} 2 \mu s / \tau_{off} 2 \mu s$ |

**Figure 3.** Surface quality of mirror blank produced by #325.**Figure 4.** *Sa* due to mesh and bonding material of wheel.

4. Effect of nano-diamond contained grinding wheels

ND is of a single crystal structure, and is easily aggregated into its clusters, as demonstrated in figure 7 [13]. Through stirred-media milling with microbeads, ND clusters have been

**Figure 5.** Surface profiles produced by #4000 wheels.**Figure 6.** Surface profile produced by #8000 metal resin bond wheel.**Figure 7.** Nano-diamond (ND) clusters. Reproduced with permission from Elsevier.

dissociated into single particles, which were then dispersed as colloidal liquid. Afterwards, the ND colloidal liquid was used to fabricate ND (1% in volume) contained grindstones. The process is detailed in figure 8 [14]. For comparison, a grindstone without ND was also fabricated. Figure 9 illustrates a tribological testing method used to evaluate the friction coefficient and

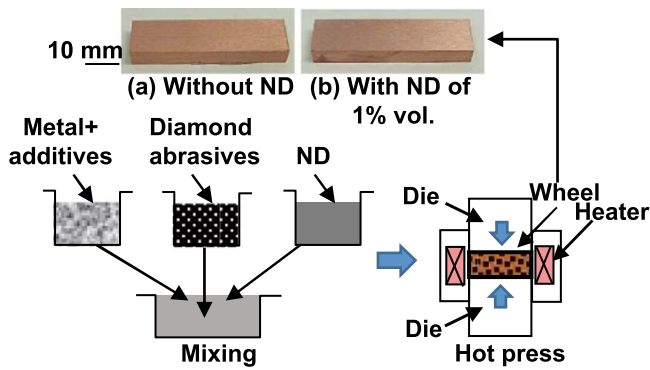


Figure 8. Fabrication process of ND contained wheel (grindstone).

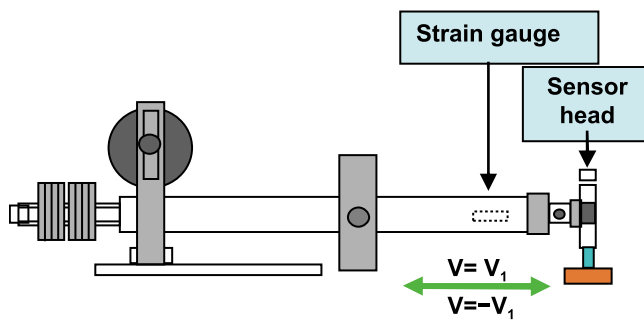


Figure 9. Tribological test evaluating friction coefficient.

its fluctuation on grindstones both with and without ND. Figure 10 [14] displays the difference in friction coefficients. The grindstone with ND exhibited lower friction coefficients with greater stability, compared to that without ND. These results suggest that an ND contained wheel can function with lower grinding force due to its superior tribological properties. Based on this finding, #20000 wheels containing ND were fabricated for the practical grinding trials of mirrors.

Grinding experiments for mirrors were then conducted by applying the fabricated #20000 wheels both with and without ND. The results confirmed that the addition of ND decreased the ground surface roughness, as presented in figure 11. The average surface roughness value without ND was 5.84 nm. Those with 2% ND, however, were able to achieve a surface roughness value that was 1/3 of those without ND. Although further research is needed to investigate its mechanisms, for the purposes of this study, it can be concluded that ND contained wheels can be applied to produce higher quality mirrors.

5. Improvement of surface quality by simultaneous grinding

In order to improve the surface quality of mirrors through the grinding process, simultaneous grinding [15] has been attempted. As displayed in figure 12 (left), mirror work pieces have been simultaneously ground together with a cemented carbide (WC-Co, Co content: 6%) ring. As a mirror work piece was placed in the central area of the jig plate, the WC-Co ring was placed in the peripheral region of the same jig plate. Using this configuration, a mirror work piece was simultaneously ground with the WC-Co

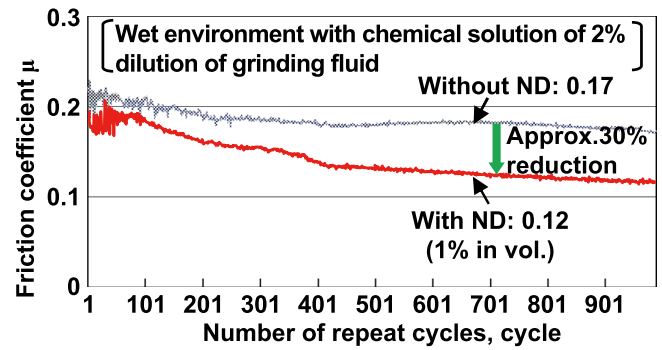


Figure 10. Reduction of friction coefficient with ND.

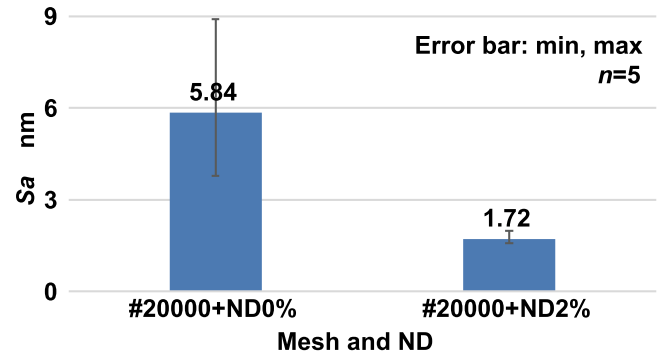


Figure 11. Reduction effect on roughness by addition of ND to wheel.

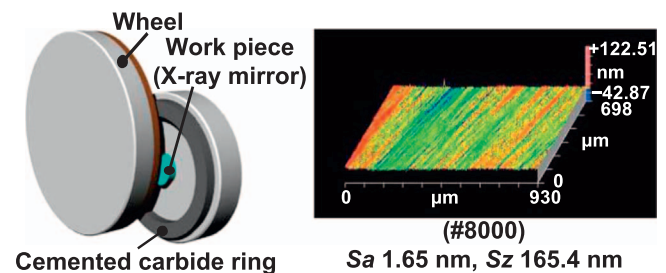


Figure 12. Simultaneous grinding method and its effect on #8000.

ring. Figure 12 (right) illustrates the surface profile produced from simultaneous grinding using a #8000 metal resin bond wheel, demonstrating its effect. The roughness example in S_a without simultaneous grinding was 6.52 nm (figure 6); however, the one with simultaneous grinding achieved 1.65 nm. The roughness values with simultaneous grinding, even with the same wheels, were lower; average S_a of 1.72 and 1.46 using #20000 wheels with ND 2% and 4%, respectively, without simultaneous grinding, compared to average S_a of 1.38 and 1.12 using the same #20000 wheels with ND 2 and 4%, but with simultaneous grinding. The surface profile examples produced from the #20000 wheels containing ND 0% and 2% are shown in figure 13. Therefore, mirrors containing ND and produced under simultaneous grinding will have weaker grinding marks.

6. Further improvement of surface quality through additional CMP

After grinding using #8000 was completed, a series of CMP [16, 17] processes were added for the purpose of removing

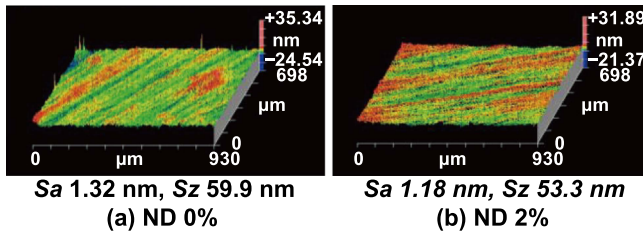


Figure 13. Surface profiles with simultaneous grinding using #20000 wheels.

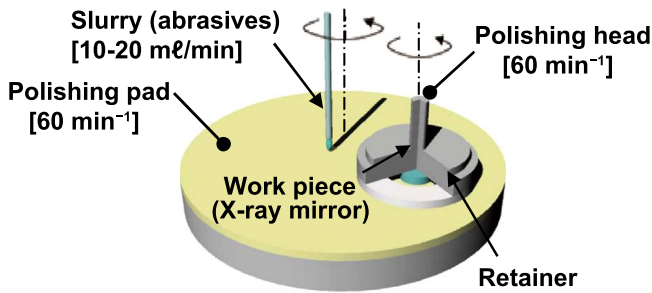


Figure 14. Employed single sided CMP method.

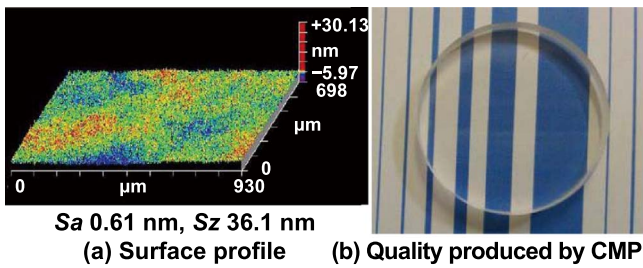


Figure 15. Surface quality after final CMP with CeO₂ slurry.

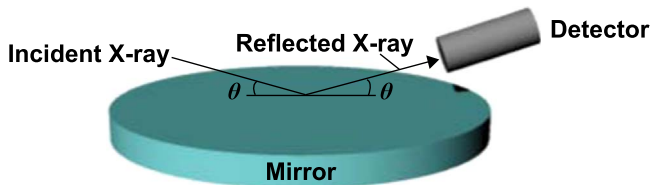


Figure 16. X-ray reflectivity evaluation.

grinding marks. A single-sided polishing method (figure 14) was employed in this experiment. For the first step, calcined ceria (CeO₂) abrasives were applied for 10 min to smooth the ground surface. Next, colloidal silica (SiO₂) and colloidal ceria were applied for polishing, for 2 min and 5 min respectively, for further smoothing. Lastly, colloidal silica was applied for 30 min for a final smoothing. Figures 15(a) and (b) display the surface profile and its top view, respectively, on the finished mirror. The mirror produced by the additional CMP processes detailed above was able to achieve an average of 0.85 nm in *Sa*.

7. Evaluation of produced x-ray total reflection mirrors

X-ray reflectivity evaluation [18] (figure 16) was conducted on mirrors produced by #325 (blank), #8000, #20000 + ND2%

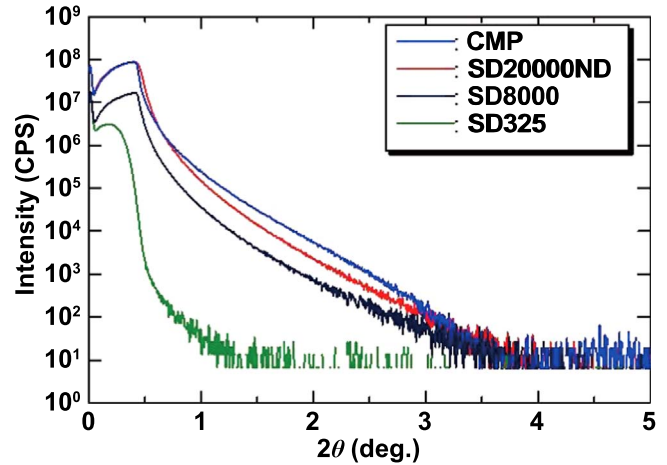


Figure 17. Evaluation of x-ray reflectivity on produced mirrors.

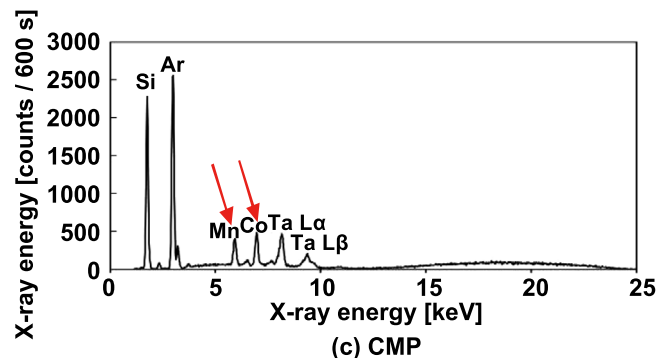
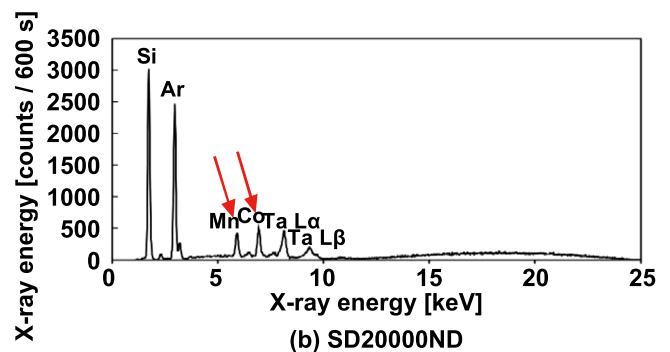
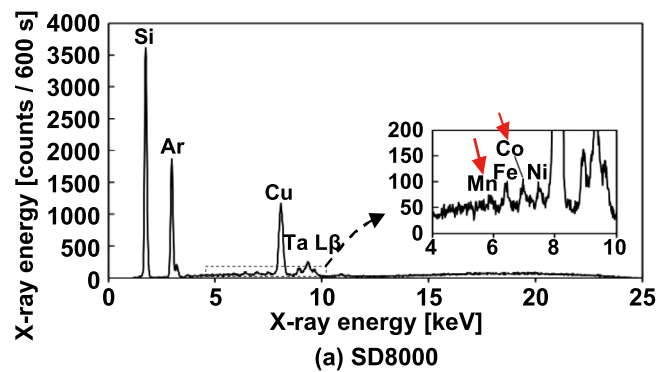


Figure 18. Evaluation of mirrors on x-ray fluorescence spectroscopy.

(hereinafter, #20000ND), and the additional CMP (hereinafter, CMP). The results are as displayed in figure 17. The mirrors produced by finer wheels exhibited higher reflectivity. CMP attained the highest reflectivity and #20000ND was a close

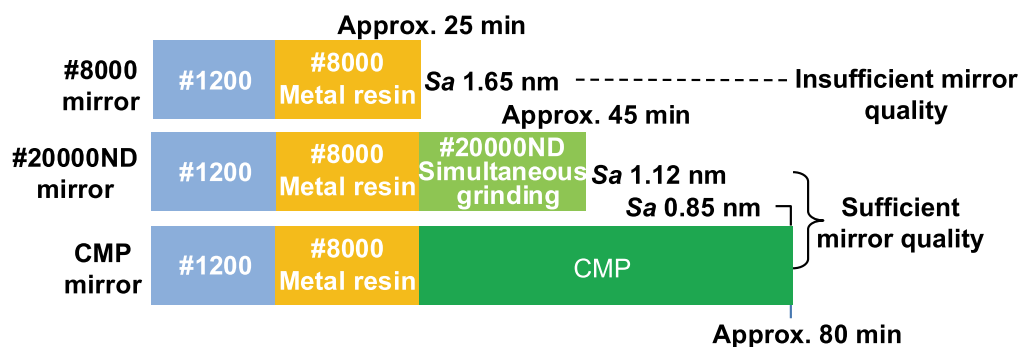


Figure 19. Process comparison for production of x-ray mirror.

second. The blank produced the lowest. After learning the above results, mirrors produced from #8000, #20000ND, and CMP were evaluated on the developed portable TXRF spectrometer for ultra-trace analysis, which compares the detection limits of elements.

Figure 18 illustrates the spectra of analytes containing 1 ng each of Mn and Co, obtained with #8000, #20000ND and CMP mirrors. These analytes were prepared by placing and drying 1 μ l drops of a standard solution that contained 1 mg/l each of Mn and Co on each mirror. As shown in figure 18(a), an Si line was detected because of the quartz glass mirror. An Ar line originating from air containing 0.9% of argon was also detected. Ta L lines originated from the x-ray tube with a tantalum anode. Ni, Cu lines are attributed to mirror contaminations. Figures 18(b) and (c) also display the detection of an Si line, an Ar line, and Ta L lines, all originating from their same respective sources as detailed above.

These analytes spectra indicate that the #8000 mirror demonstrate low detecting sensitivities for both elements. The detection limits of Mn and Co with the #20000ND mirror were 31 pg and 25 pg respectively, and those with the CMP mirror were 35 pg and 30 pg respectively. The difference in the detection limits between #20000ND and CMP mirrors may derive from variations that can arise in the measurement process. The results signify that the quality of the #20000ND mirror is sufficient to be practically applied to the portable spectrometer [11]. Figure 19 compares the finishing process among the three mirrors. Therefore, the #20000ND mirror can be fabricated through an adequate process combination of consistent grinding sequence to provide sufficiently high performance with both abbreviated process length and time.

8. Conclusions

This study aimed to establish a dedicated finishing process for creating high-quality surfaces for total reflection mirrors that can be applied to the portable TXRF spectrometer. The experiment has successfully demonstrated that the final finishing through simultaneous grinding of #20000ND in a

consistent grinding sequence can both effectively and practically generate sufficiently high mirror quality, which enables detection limits of 31 pg and 25 pg for Mn and Co, respectively.

ORCID iDs

Hiroshi Kasuga <https://orcid.org/0000-0001-9269-6313>

References

- [1] Mimura H *et al* 2007 Efficient focusing of hard x-rays to 25 nm by a total reflection mirror *Appl. Phys. Lett.* **90** 051903
- [2] Kunimura S and Kawai J 2010 Polychromatic excitation improves detection limits in total reflection x-ray fluorescence analysis compared with monochromatic excitation *Analyst* **135** 1909
- [3] Perlman E S, Rappaport S A, Christiansen W A, Ng Y J, DeVore J and Pooley D 2015 New constraints on quantum gravity from x-ray and gamma-ray observations *Astrophys. J.* **805** 10
- [4] Poyneer L A, McCarville T, Pardini T, Palmer D, Brooks A, Pivovarov M J and Macintosh B 2014 Sub-nanometer flattening of 45 cm long, 45 actuator x-ray deformable mirror *Appl. Opt.* **53** 3404
- [5] Yin L and Huang H 2008 Brittle materials in nano-abrasive fabrication of optical mirror-surfaces *Prec. Eng.* **32** 336
- [6] Namba Y, Kobayashi H, Suzuki H, Yamashita K and Taniguchi N 1998 Ultra-precision surface grinding of chemical vapor deposited silicon carbide for x-ray mirrors using resinoid-bonded diamond wheels *Ann. CIRP* **48** 277
- [7] Yamaguchi H, Riveros R E, Mitsuishi I, Takagi U, Ezoe Y and Yamasaki N 2010 Magnetic field-assisted finishing for micropore x-ray focusing mirrors fabricated by deep reactive ion etching *Ann. CIRP* **59** 351
- [8] Ohmori H and Nakagawa T 1990 Mirror surface grinding of silicon wafers with electrolytic in-process dressing *Ann. CIRP* **39** 329
- [9] Mori Y, Yamauchi K and Endo K 1987 Elastic emission machining *Prec. Eng.* **9** 123
- [10] Mimura H, Ohmori H and Yamauchi K 2012 Development of focusing system for x-ray free electron laser *Key Eng. Mater.* **516** 251
- [11] Kunimura S, Kudo S, Nagai H, Nakajima Y and Ohmori H 2013 Portable total reflection x-ray fluorescence spectrometer with small vacuum chamber *Rev. Sci. Instrum.* **84** 046108

- [12] Klockenkämper R and Bohlen A V 2015 *Total-Reflection X-ray Fluorescence Analysis and Related Methods* (New York: Wiley)
- [13] Eidelman E D, Siklitsky V I, Sharonova L V, Yagovkina M A, Vul A Y, Takahashi M, Inakuma M and Ōsawa E 2005 A stable suspension of single ultra-nanocrystalline diamond particles *Diam. Relat. Mater.* **14** 1765
- [14] Kasuga H, Kato T, Itoh N, Kameyama Y and Ohmori H 2011 Grinding characteristics of sapphire (0001) surface with metal bonded grinding wheel containing nano-diamond *Trans. MIRAI Micro-Fabr. Green Technol.* **2** 27
- [15] Ohmori H, Marinescu I D and Katahira K 2011 *Electrolytic In-Process Dressing (ELID) Technologies: Fundamentals and Applications* (New York: CRC Press)
- [16] Jeong H D, Park K H and Cho K K 2007 CMP pad break-in time reduction in silicon wafer polishing *Ann. CIRP* **56** 357
- [17] Kurokawa S, Toyama T, Hayashi T, Suda E and Tokuda J 2017 Controllable CMP of oxide film by using colloidal ceria slurry *Proc. Int. Conf. Planarization/ CMP Technol. ICPT2017* p 177
- [18] Daillant J and Gibaud A 2009 *X-ray and Neutron Reflectivity, Principles and Applications* (Berlin: Springer)